EVALUATION OF DRY SLIDING WEAR CHARACTERISTICS AND CONSEQUENCES OF CAST Al-Si-Mg-Fe ALLOYS

A.Chennakesava Reddy[*] and S. Madhava Reddy[**]

In the present study, dry sliding wear characteristics of Al-Si-Mg-Fe alloy have been investigated. The influence of variables viz: contact time, sliding speed, and normal pressure on wear behaviour were studied. The results conclude that the wear loss increases with increase in contac time and normal pressure and decreases with sliding speed. The wear mechanisms include abrasive, adhesive, slip, melt-wear and oxidative phenomena. The consequences of wear were work hardening, and diffusion of microstrucutral constituents.

Keywords: dry sliding wear, contact time, sliding speed, normal pressure

1. INTRODUCTION

Use of cast Al-alloys as a tribological component in recent years, has been expanding widely in aeronautical, automobile and general industries (Odani 1994). Applications requiring enhanced friction and wear performances, include brake rotors, engine blocks and cylinder liners, connecting rods and pistons, gears, valves, pulleys, suspension components, etc (Noguchi and Fukizawa 1993). Depending upon the applications, these alloys may be sand cast, investment cast and die cast. The tribological behaviour can be evaluated in terms of wear characteristics. The wear characteristics of these alloys depend upon the material morphology such as composition, size, shape and distribution of micro constituents and service conditions such as load, contact surface, contact time and sliding speed (Sarkar 1976). Modifiers are added to eutectic and hypereutectic Al-Si alloys to refine eutectic Si from angular platelets to fine fibers. Good modification can be obtained by the use of strontium or sodium (Kori et al 2000). Numerous studies have been reported on the wear behaviour of Al-Si alloys.

The present work is on the evaluation of wear characteristics and consequences of cast Al-Si-Mg-Fe alloys.

[*]Professor in Mechanical Engineering, JNTU College of Engineering, Anantapuram – 515 002, Anfhra Pradesh, India; and is the corresponding author, E-nail: dr_acreddy@yahoo.com

[**]Associate Professor, Department of Mechanical Engineering, Mahatma Gandhi Institute of Technology, Gandipet; Hyderabad, India, E-mail: smrmesh@gmail.com

2. EXPERIMENTAL PROCEDURE

An Al-Si-Mg-Fe alloys were melted in an oil-fired furnace. The melting losses of aluminum and magnesium were taken into account while preparing the charge. During melting, the charge was fluxed with coveral-11 (a Foseco company product) to prevent dressing. The molten metal was then degasified by tetrachlorethane (in solid form) using a plunger ending in a small inverted crucible. The melt was also modified with strontium and refined with Al-Ti master alloy in the crucible before pouring. The crucibles were made of graphite.

The dross removed melt was finally gravity poured into the preheated sand mould, investment shell, and metal die. The cavity shape is cylindrical in all the methods of casting.

A pin on disc type friction and wear monitor (ASTM G99) was employed to evaluate the friction and wear behaviour of Al-Si-Mg-Fe alloys against hardened ground steel (En32) disc. Wear test pins of 6mm diameter and 20mm length were prepared. Wear tests include the measurement of:

1. Weight loss using electronic weighing balance with accuracy up to 0.1 mg,
2. Temperature of pin using thermocouple, and
3. Friction force with data acquisition system

An investigation has been carried out to study the effects of sliding speed, contact time, normal pressure, and casting procedure of Al-Si-Mg-Fe alloys on the wear characteristics. The mechanical properties and metallurgical morphology were investigated to evaluate the wear behaviour of these alloys. EDX analysis was also carried out to find the major elements present in the worn surface of the wear specimens. Each experiment was repeated twice and the average values of wear characteristics were plotted against the process variables.

3. RESULTS AND DISCUSSION

Mechanical Properties of Al-Si-Mg-Fe Alloys

The mechanical properties of Al-Si-Mg-Fe alloy (7.83%Si-0.7%Mg-0.3%Fe-0.03%Cu-0.015%Mn-0.083%Zn-0.006%Pb-0.01%Sr-0.004Ti-0.0005%Ni-remainderAl) are given in Table-1. The mechanical properties of die cast alloy are superior to investment cast and sand alloys. The reason could be the fine grain structure in the die cast alloys. The grain structure in the casting is influenced by the solidification process. The solidification time was short for the die castings whereas it was long for the sand casting and intermediate for the investment castings. The prolonged solidification retards the nucleation and promotes the growth of crystals.

Table-1: Mechanical Properties of Al-Si-Mg-Fe alloys

Mechanical properties	Sand cast	Investment cast	Die cast
Tensile strength, N/mm^2	199.52	213.64	234.11
% Elongation	9.1	9.8	10.2
Hardness (surface), BHN	71	75	87

The microstructure of sand cast and investment cast specimens consist of large elongated α-Al dendrites and plate-like eutectic silicon induces poor mechanical properties. The intermetallic compounds are in large in size.

The grain refiner Al-Ti and strontium modifier together with fast solidification in the die cast specimens convert large elongated α-Al dendrites into fine α-Al equiaxed dendrites and plate-like silicon into fine particles resulting in the improved mechanical properties. The sand casting resulted with coarse grain structure in the castings due to slow solidification process. The castings produced by the investment casting have intermediate grain size having the lower limit of die castings and the upper limit of sand castings (Figure 1).

The reaction during the solidification of alloy (7.83%Si-0.7%Mg-0.3%Fe-0.03%Cu-0.015%Mn-0.083%Zn-0.006%Pb-0.01%Sr-0.004Ti-0.0005%Ni-remainderAl) may be as follows:

Figure 1: Microstructures of Al-Si-Mg-Fe alloys produced by (a) sand cast (b) investment cast, and (c) die cast processes

$$L \rightarrow Al + Si + Mg_2Si + Al_{15}Mn_3Si_2 + Al_6FeSi + Al_5Mg_8Cu_2Si_6 \qquad \ldots(1)$$
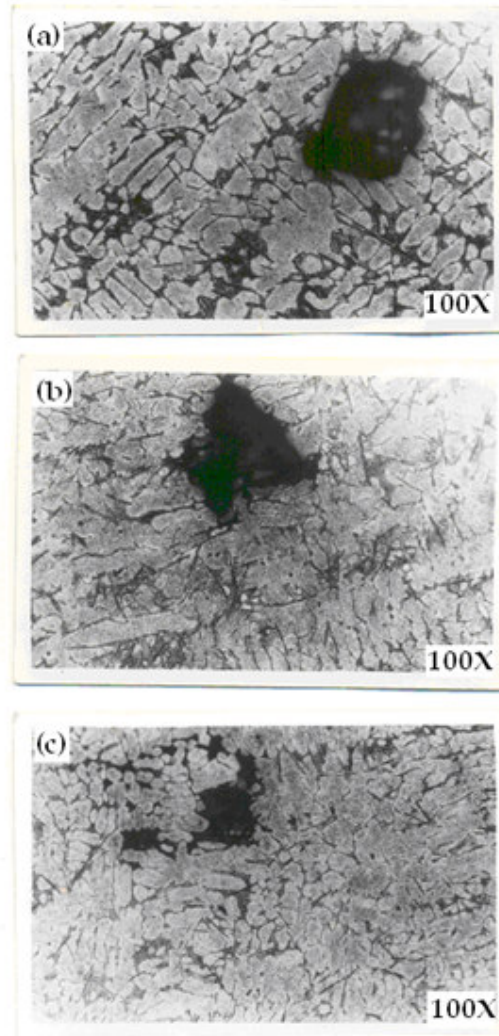
where, L is the liquid melt.

Zn does not form any detectable phase, Sn and Pb if present together with Mg, tend to enter into Mg_2Si phase. The solubility of Mn in aluminium is reduced by the presence of Fe and Si leading the formation of intermetallic compounds. The characteristics of phases observed by the optical microscopy are given Table-2.

Table-2: Characteristics of phases	
Phase	**Characteristics**
α-Al	Dendrites
Si	Grey
Mg_2Si	Black
$Al_{15}Mn_3Si_2$	Brown chinese script
Al_6FeSi	Needles
$Al_5Mg_8Cu_2Si_6$	Needles

The variations, which are observed in the present study, can be attributed to the combined effect of refinement, modification, and the solidification behaviour of Al-Si-Mg-Fe alloy. Therefore, the wear characteristics of Al-Si-Mg-Fe alloy depend on the microstructure and type of casting method.

3.2 Effect of Contact Time, Sliding Speed, And Normal Pressure on Wear

The influence of contact time is shown in figure 2. It can be seen that the specimens produced by the sand and investment casting methods, wear out faster than those produced by the die casting method. The wear resistance of specimens produced by the investment casting method is slightly better than those obtained by the sand casting method. It is also observed that a

Figure 2: Influence of contact time on wear.

Note: The normal pressure and sliding speed are respectively, 0.75Mpa and 2m/sec.
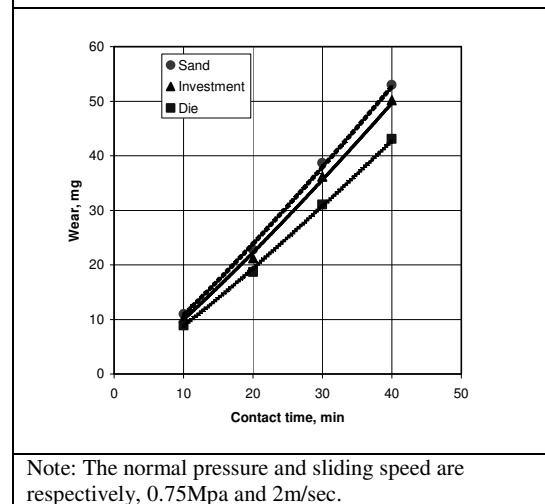
general trend of increase in wear is with increase in contact time. The major wear mechanisms are abrasive and adhesive in nature. The abrasion and adhesion are cumulative with prolonged contact time of wear specimen with the abrasive disc (for the purpose of wear test, the disc surface was

abraded against 800 grade silicon carbide polishing paper and cleaned with acetone and dried before each test). The mathematical relation between wear and contact time is given by

$$w_s = 0.7772t^{1.1429}$$
$$w_i = 0.6962t^{1.1567} \qquad \ldots(2)$$
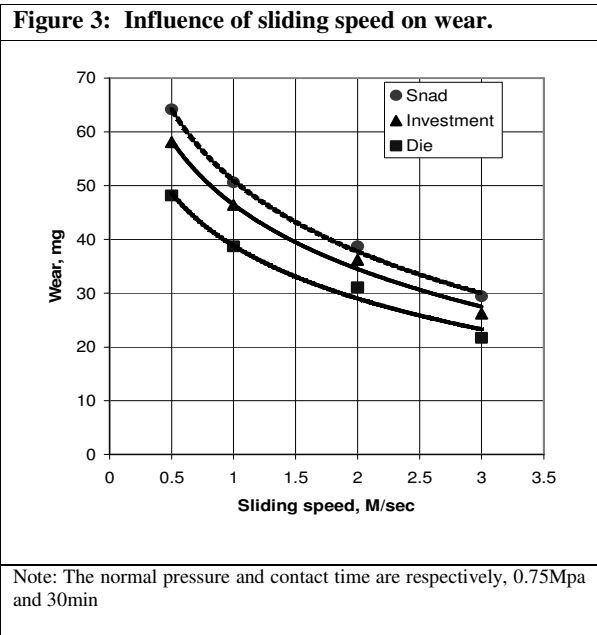$$w_d = 0.6315t^{1.1425}$$

where,

w_s is the wear of sand castings, mg

w_i is the wear of investment castings, mg

w_d is the wear of die castings, mg

t is the contact time, min

The influence of sliding speed is illustrated in figure 3. It can be seen that the wear loss decreases with increase in the sliding speed in all the specimens. Initially, the seizure is dominant resulting high wear. As the sliding speed progresses the detachment of metal is decelerated. At slow speeds the wear mechanism is abrasive in nature. The adhesive mechanism does not play significant role in the wear mechanism. As the sliding speed increases, the slip phenomena also appears. At high sliding speeds the slip phenomena dominates the abrasive mechanism consequently resulting low wear. The wear curves are parallel. The relative distance between the curves is on account of grain size, microstructural constituents, and mechanical properties. The mathematical relation between wear and sliding speed is given by:

Figure 3: Influence of sliding speed on wear.

Note: The normal pressure and contact time are respectively, 0.75Mpa and 30min

$$w_s = -19.082(\ln v) + 50.97$$
$$w_i = -17.270(\ln v) + 46.47 \qquad \ldots(3)$$
$$w_d = -14.137(\ln v) + 38.81$$

where, v is the sliding speed, m/sec

The relation between wear and sliding speed is logarithmic in nature. The die cast specimens have better wear resistance than the sand cast and investment specimens.

The influence of normal pressure on wear is shown in figure 4. The wear loss increases with increasing normal pressure in all the specimens. However, the combined effect of refinement, modification, and solidification process shows less wear loss in the die cast specimens when compared to that in the sand cast and investment cast specimens. The grain refiner (Al-Ti master alloy) to Al-Si-Mg-Fe alloy significantly refines the coarse columnar α-Al dendrites to fine

Figure 4: Influence of normal pressure on wear.

Note: The contact time and sliding speed are respectively, 30min and 2m/sec.
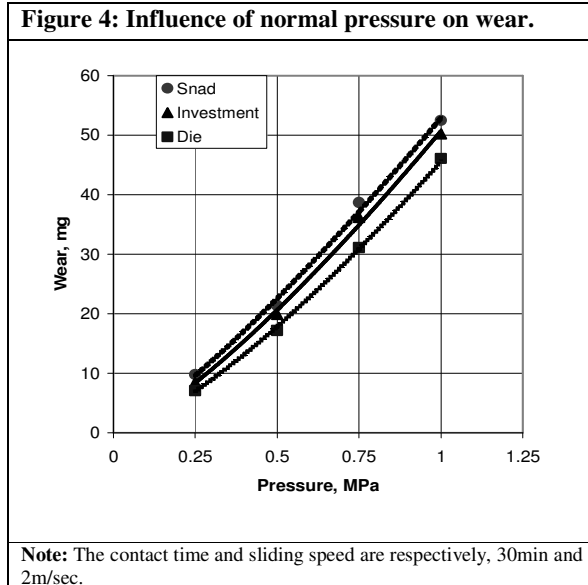
equiaxed α-Al dendrites. The grain refiner is responsible for generating several nucleating sites in the melt during the solidification process. The strontium modifier changes the plate-like eutectic silicon to fine particles. The result of refinement and modification is improved strength and toughness.

In the die casting method, the solidification process was fast due to rapid removal of heat from the metal die. In the sand casting method, the solidification process was delayed because the heat removal from the sand mould takes long duration than the metal die used for die casting process. In the investment casting method, the investment shell was prepared from the slurry prepared from the colloidal silica binder and zirconia filler material and each layer of slurry was stuccoed with fine silica sand. The shell thickness was 15mm. The distance of heat travel from the center of the casting in the investing casting method was shorter than the in the sand casting method. Therefore, the resulting microstructure in the investment cast specimens is relatively finer than that in the sand cast specimens and is coarser than that in die cast specimens. The fine grain structure in the specimens results in better mechanical properties.

The intermetallic compounds are small in size and randomly distributed in the die cast specimens whereas the intermetallic compounds are large in size and clustered in the sand cast and investment cast specimens. The intermetallic compounds are brittle in nature. The wear loss is

countable for the amount of intermetallic compounds detached from the specimens during the test. At low normal pressure, the wear mechanism is abrasive and adhesive in nature. As the normal pressure increases the wear mechanism also includes melt wear because of the rise in temperature on the localized wear surface, resulting rapid metal loss from the specimens. The mathematical relation between wear and normal pressure is given by

$$w_s = 52.853p^{1.2283}$$
$$w_i = 50.706p^{1.2962} \qquad \qquad \text{...(4)}$$
$$w_d = 45.546p^{1.3527}$$

where, p is the normal pressure, MPa

3.3 Effect of Contact Time, Sliding Speed, And Normal Pressure on Frictional Force

The influence of contact time on frictional force is shown in figure 5. The frictional force increases with increasing of contact time up to 30 min and then decreases with further increase in the contact time for all the specimens. The increase in the frictional force may be attributed to the dominant role of abrasive mechanism, which is responsible for dry wear up to 30 min of contact time. The decrease in the frictional force may be ascribed to the dominant role of adhesive mechanism, which is accountable for

Figure 5: Influence of contact time on frictional force.

Note: The normal pressure and sliding speed are respectively, 0.75Mpa and 2m/sec.
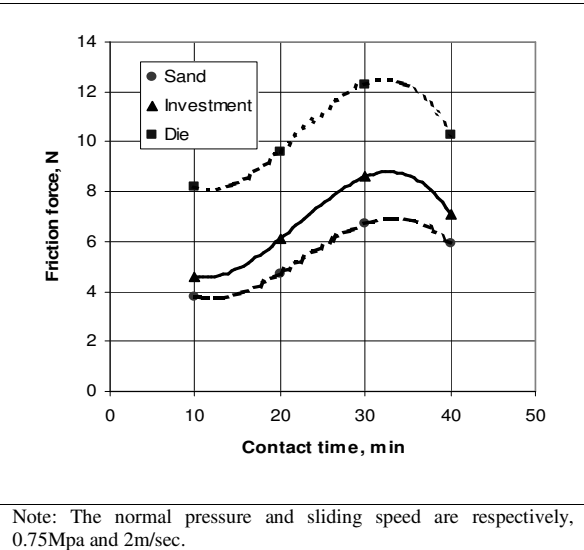
the formation of viscous layer between the pin and abrasive disc. The viscous layer reduces the coefficient of friction and subsequently reduces the frictional force developed during the long contact periods.

The frictional force is higher for die cast specimens than that for sand cast specimens. The reason could be due to the presence of fine grain structure in the die cast specimens and the coarse grain structure in the sand cast specimens. The fine grains have greater surface area per unit volume than the large and irregular grains. The frictional force generated in the investment cast

specimens is intermediate to the sand cast and die cast specimens. The mathematical relation between contact time and frictional force is given by

$$F_s = -0.0007t^3 + 0.0445t^2 - 0.79t + 7.9$$
$$F_i = -0.0008t^3 + 0.055t^2 - 0.9167t + 9.1 \qquad \ldots(5)$$
$$F_d = -0.001t^3 + 0.0665t^2 - 1.155t + 14.1$$

where,

F_s is the frictional force of sand castings, N

F_i is the frictional force of investment castings, N

F_d is the frictional force of die castings, N
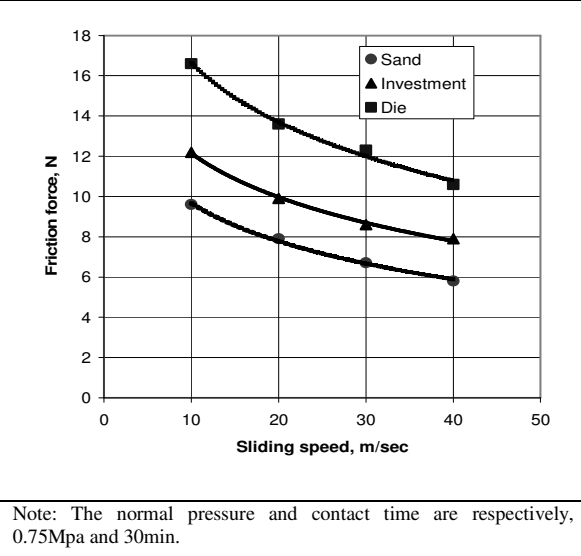
t is the contact time, min.

The influence of sliding speed on frictional force is demonstrated in figure 6. The frictional force decreases with increasing of sliding speed for all the specimens. This is in fact, a general phenomenon because the dynamic coefficient of friction is lower than the static coefficient of friction. Furthermore, the slip phenomena appearing between the pin and the abrasive disc lowers the frictional force. The mathematical relation between sliding speed and frictional force is given by

Figure 6: Influence of sliding speed on frictional force.

Note: The normal pressure and contact time are respectively, 0.75Mpa and 30min.

$$F_s = -2.7286(\ln v) + 15.951$$
$$F_i = -3.1417(\ln v) + 19.38 \qquad \ldots(6)$$
$$F_d = -4.2005(\ln v) + 26.284$$

where, v is the sliding speed, m/sec.

The influence of normal pressure on frictional force is shown in figure 7. It can be seen that a general trend of increase in frictional force with increase in normal pressure. The frictional force is directly proportional to the normal pressure applied on the pin. The die cast specimens have higher frictional forces developed than the sand cast specimens. The frictional force developed is proportional to the hardness value of the material and is inversely proportional to the material

loss. The material loss is more for the sand cast specimens. The mathematical relation between the normal pressure and frictional force is given by

$$F_s = 1.4022e^{2.0971p}$$
$$F_i = 2.3672e^{1.7135p} \qquad …(7)$$
$$F_d = 4.412e^{1.4274p}$$

where, p is the sliding speed, MPa.

The frictional force is exponential to the normal pressure applied on the specimen.

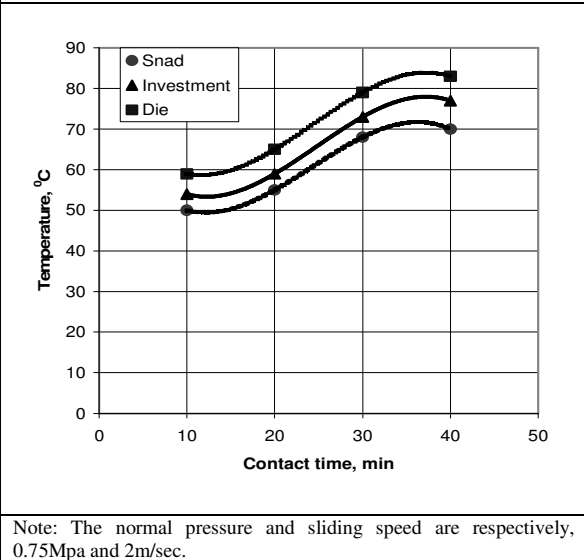**Figure 7: Influence of normal pressure on frictional force.**

Note: The contact time and sliding speed are respectively, 30min and 2m/sec.
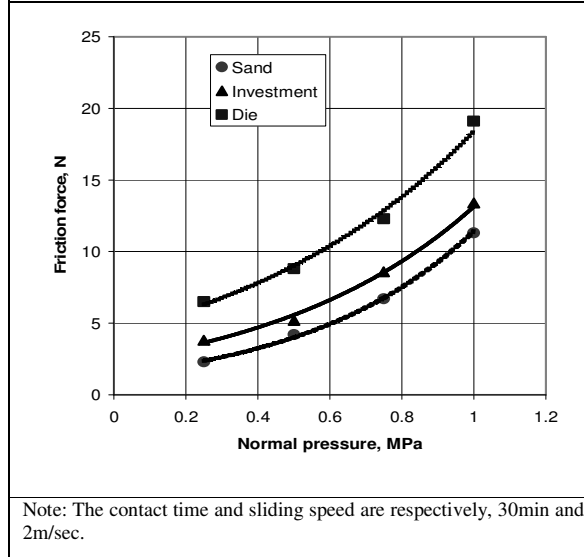
3.4 Effect of Contact Time, Sliding Speed, And Normal Pressure on Temperature

The influence of contact time on the temperature generated in specimen is shown in figure.8. The temperature rise in the specimen is proportional to its contact time with the abrasive disc during the wear test. With the increase of contact time the corresponding frictional temperature rises steadily due to the increased conversion of frictional energy into heat energy. The trend of temperature rise in the specimen is same as that is observed with the amount of frictional force developed (figure 5). The mathematical relation between contact time and temperature rise in the specimen is given by

Figure 8: Influence of contact time on temperature rise.

Note: The normal pressure and sliding speed are respectively, 0.75Mpa and 2m/sec.

$$T_s = -0.0032t^3 + 0.23t^2 - 4.1833t + 72$$
$$T_i = -0.0032t^3 + 0.235t^2 - 4.3333t + 77 \qquad …(8)$$
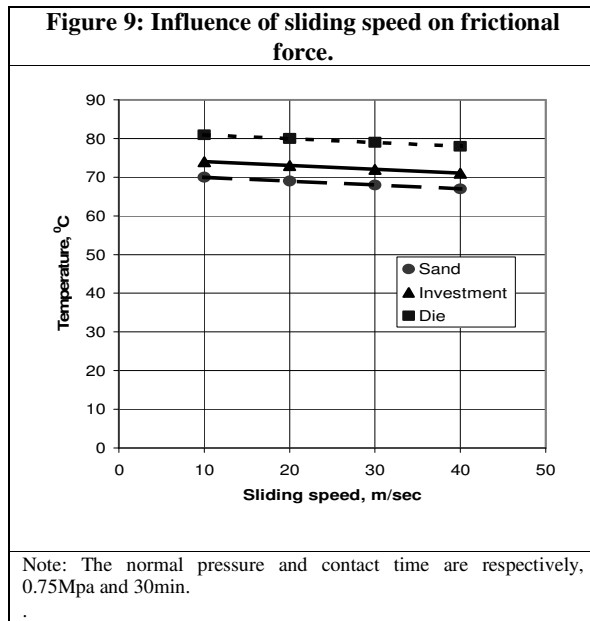$$T_d = -0.003t^3 + 0.22t^2 - 3.0t + 79$$

where,

T_s is the temperature rise of sand castings, ^0C

T_i is temperature rise of investment castings, ^0C

T_d is the temperature rise of die castings, ^0C

t is the contact time, min.

The influence of sliding velocity on the temperature generated is illustrated in figure 9. It is clearly observed that there is no influence of sliding speed on the temperature rise in the specimen. It may be attributed to the slip phenomena, which creates new interface between the specimen and the abrasive disc continuously. Consequently, there may be interruption for the temperature flow into the specimen because the heat experienced interface is passed on by the new and cold interface. The mathematical relation between sliding speed and temperature rise in the specimen is given by

Figure 9: Influence of sliding speed on frictional force.

Note: The normal pressure and contact time are respectively, 0.75Mpa and 30min.

$$T_s = -0.1v + 71$$
$$T_i = -0.1v + 75 \qquad\qquad …(9)$$
$$T_d = -0.1v + 82$$

where, v is the sliding speed, m/sec.

The mathematical relation between the sliding speed and the temperature rise is linear. The gradient of the curves is 0.1 only for all the specimens. The temperature rise due to change in sliding speed is negligible.

The influence of normal pressure on the temperature rise of specimens is demonstrated in figure 10. The temperature rise in all the specimens increases with increasing of normal pressure on the specimens. Moreover, the increase in the normal pressure on the specimen results the plastic deformation of the wearing surface and subsequently rise in frictional temperature. The temperature rise is exponential of normal pressure on the specimen. This may be on account of

wear mechanism consisting of abrasive, adhesive, and melt wear phenomena. The mathematical relation between the normal pressure and temperature rise in the specimens is given by

$$T_s = 30.495e^{1.103p}$$
$$T_i = 35.550e^{1.06p} \qquad \ldots(10)$$
$$T_d = 33.061e^{1.025p}$$

where, p is the sliding speed, MPa.

4. CONSEQUENCE OE WEAR IN Al-Si-Mg-Fe ALLOYS

There is a metal loss due to wear by the variation of variables viz: contact time, sliding speed, and normal pressure. The

Figure 10: Influence of normal pressure on temperature rise.

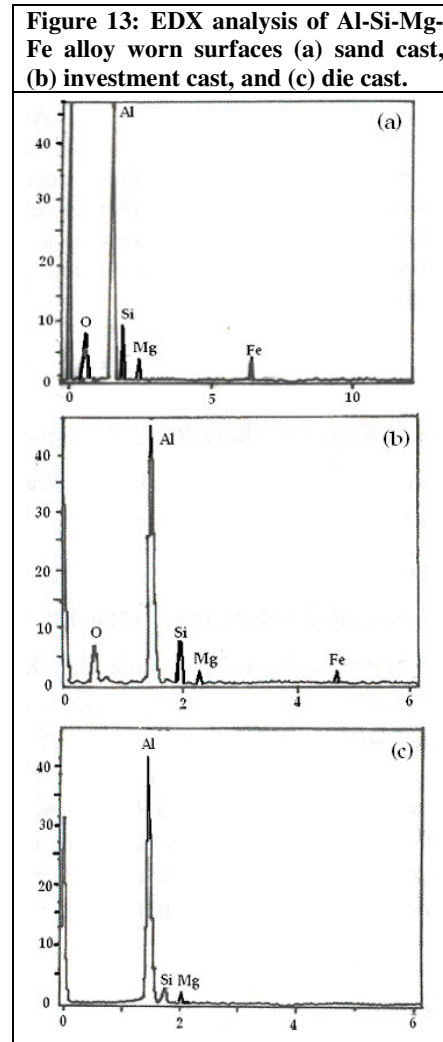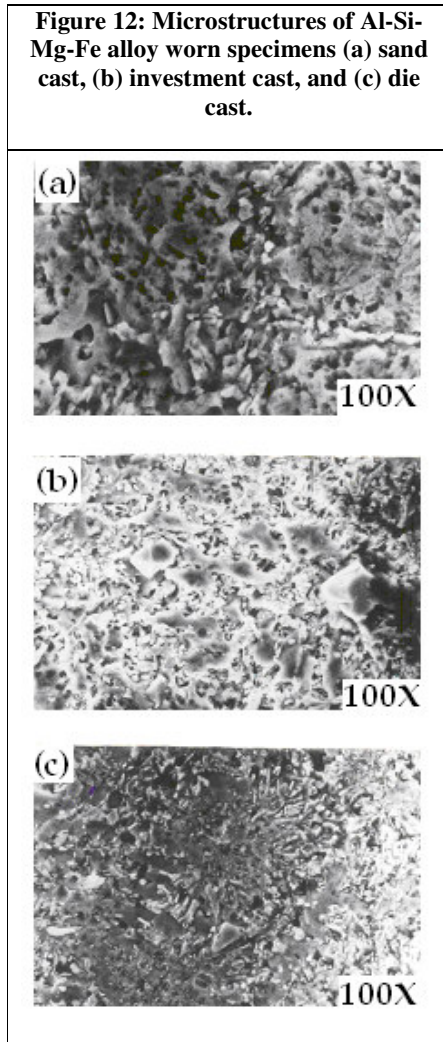Note: The contact time and sliding speed are respectively, 30min and 2m/sec.

amount of metal loss depends upon the strength of contact time, sliding speed and normal pressure, and the pertinent wear mechanisms (abrasive / abrasive / slip / melt-wear) thereon.

It is also known that the wear behaviour is greatly influenced by the microstructural morphology of Al-Si-Mg-Fe alloy and the method of casting. It is essential to know the consequence of wear in Al-Si-Mg-Fe alloys. The purpose of post-wear evaluation is to focus the changes that are brought in the worn specimens in terms of mechanical properties, microstructure, and worn-surface pattern.

The worn specimens are not length

Figure 11: Hardness values of worn specimens

enough for tensile testing to evaluate tensile strength and %elongation. Therefore, the worn specimens were tested for hardness only. The change in hardness of the worn specimens is shown in figure 11. It can be seen that the hardness values increase after wear test. The increase in
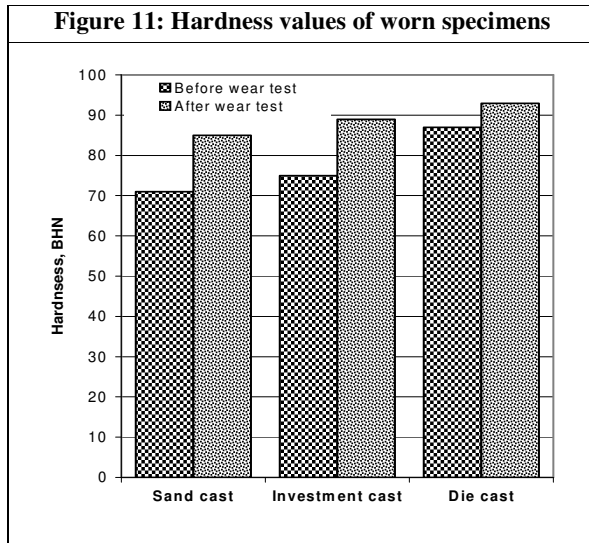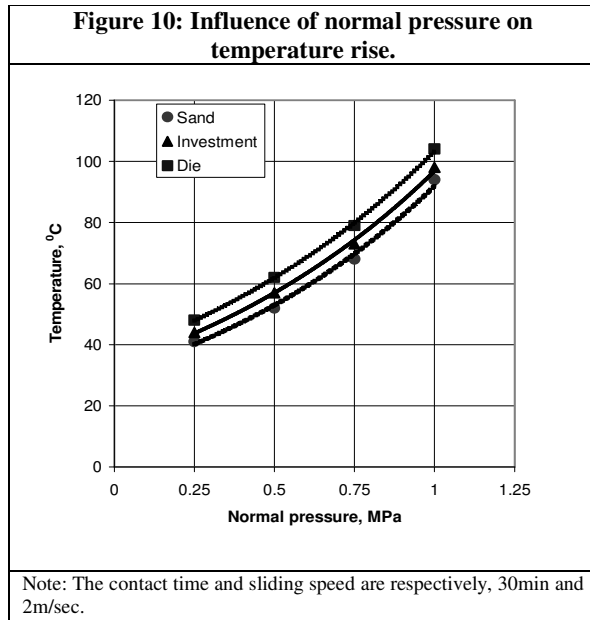
hardness in the worn specimens may be attributed to the work (strain) hardening and the frictional temperature.

Figure 12: Microstructures of Al-Si-Mg-Fe alloy worn specimens (a) sand cast, (b) investment cast, and (c) die cast.	Figure 13: EDX analysis of Al-Si-Mg-Fe alloy worn surfaces (a) sand cast, (b) investment cast, and (c) die cast.

Figure 12: Microstructures of Al-Si-Mg-Fe alloy worn specimens (a) sand cast, (b) investment cast, and (c) die cast.

Figure 13: EDX analysis of Al-Si-Mg-Fe alloy worn surfaces (a) sand cast, (b) investment cast, and (c) die cast.

The microstructures of worn specimens are revealed in figure 12. The grains become finer owing to the work hardening. There is also diffusion across the grain boundaries due to the frictional temperatures and strain hardening. The frictional temperatures rise in the worn specimens on account of increased conversion of frictional energy into heat energy. The frictional temperatures and plastic deformations of the wearing surface result in the movement of dislocation in the wearing layers. The frictional temperatures also result in tempering which in turn soften the structure. The increase in hardness values of worn specimens indicates that the

work hardening effect dominates the softening effect. The softening of structure in the wearing specimens aids in the diffusion across the grain boundaries.

Figure.13 shows the EDX analysis of worn surfaces of Al-Si-Mg-Fe alloy. EDX analysis showed that the worn surfaces contain Al, Si, Mg, Fe, O, and indicating the presence of Fe_2O_3, Al_2O_3, and MgO. This confirms that the wear mechanism also consists of oxidative phenomena.

5. CONCLUSIONS

The following are drawn from the present work as follows:

1. The wear resistance increases with the addition of grain refiner (Al-Ti master alloy) and the modification by strontium.
2. The wear loss increases with increase in normal pressure at constant contact time and at constant sliding speed.
3. The wear loss increases with increasing contact time at constant normal pressure and at constant sliding speed.

4. The wear loss decreases with increasing sliding speed at constant normal pressure and at constant contact time.
5. Al-Si-Mg-Fe alloy exhibits abrasive, adhesive, slip, melt-wear and oxidative mechanisms.
6. The consequences of wear work hardening and diffusion microstrucutral constituents of Al-Si-Mg-Fe alloy.

REFERENCES:

1. Odani, Y. (1994), "Aluminium Alloys", Metal Powder Report, 49, 36-40.
2. Noguchi, M. & Fukizawa, K. (1993), "Aluminium composite cylinder liners", Advances in Materials and Processes, 143(6), 19-21.
3. Sarkar, A D. (1976), "Wear of metals", Pregaman Press, England, 1976.

4. Kori. S A, Murty. B S, and Chakraborty. M. (2000), "Development of an efficient grain refiner for Al-7Si alloy and its modification with strontium", Materials science and engineering, 25, 94-104.